Research Paper
Computational Methods for Differential Equations
http://cmde.tabrizu.ac.ir
Vol. *, No. *, *, pp. 1-20
DOI:10.22034/cmde.2025.65535.3018

An investigation of fractional Typhoid Fever disease model using homotopy decomposition method

Nisha Meena[1], Yogesh Khandelwal[1], Lokesh Kumar Yadav[2], Murli Manohar Gour[2], and Sunil Dutt Purohit[3,*]

[1]Department of Mathematics, Jaipur National University, Jaipur, India.

[2]Department of Mathematics, Vivekananda Global University, Jaipur, India.

[3]Department of HEAS (Mathematics), Rajasthan Technical University, Kota, India.

Abstract

Typhoid fever remains a major public health threat on a global scale. It is mainly transmitted by contaminated food and water, particularly in places with poor sanitation. In this study, we are building a fractional order mathematical model to investigate the transmission dynamics of typhoid fever employing the Riemann–Liouville fractional derivative operator. The model is analyzed using the homotopy decomposition method (HDM) combined with the modified derivative β, which allows the incorporation of memory effects without requiring linearization, discretization, or restrictive assumptions, thus reducing computational complexity. The fixed-point theory (FPT) is used to prove the existence and uniqueness of the proposed model. MATLAB simulations are performed to graphically analyze the model's behavior, demonstrating how fractional parameters influence disease progression. The novelty of the present study lies in the detailed analysis of the effects of various epidemiological parameters on the dynamics of the disease, which are effectively illustrated through comprehensive graphical solutions. The results offer valuable insights for designing effective disease control strategies and contribute to the advancement of fractional epidemiological modeling with potential applications in public health policy and clinical research.

Keywords. Fractional typhoid fever model, Fractional calculus, Homotopy decomposition approach.

2010 Mathematics Subject Classification. 34A08; 34D20; 34K60; 92C50; 92D30.

1. Introduction

Typhoid fever, which is common in places with poor sanitation around the world, is contracted by eating contaminated food or water (stool) contaminated with salmonella bacteria (Salmonella typhi) [40, 54]. The main symptoms of the condition include fever that progressively increases to $40^{\circ}C$, anorexia, headaches, exhaustion, and insomnia [19, 40, 49, 54]. In addition to fever, there may be gastrointestinal problems (constipation, diarrhea, or vomiting) [14, 33, 44]. The signs and symptoms may last for a few weeks. The infected host contributes to the transmission of the disease, although they may not always show any symptoms. Antibiotics are the cornerstone of typhoid fever treatment, and several cases of evolution can be fatal in 10% of infected individuals if treatment is not received. An estimated 11 to 21 million cases of typhoid fever and approximately 128,000 to 161,000 deaths occur annually, compared to an estimated 6 million cases of paratyphoid fever and 54,000 fatalities.

Prevention and control strategies for typhoid fever include antibiotic treatment, standard hygiene precautions related to stool handling, vaccination, improved environmental sanitation, and access to clean water [14]. Medical treatment typically leads to symptom relief within four weeks; however, incomplete treatment may result in symptom recurrence [16]. The first typhoid vaccine was developed over a century ago, and oral and injectable vaccines are now available. The injectable Vi polysaccharide vaccine provides approximately 65% protection and is considered safe. The Ty21a oral vaccine, approved for children aged two years and older, is available in liquid form but is generally more expensive than the injectable option [18].

Received: 19 January 2025 ; Accepted: 28 July 2025.
∗ Corresponding author. Email: sunil_a_purohit@yahoo.com.

Musa et al. [42] examined the dynamics of the spread of the typhoid fever epidemic. Their model assesses the impact of public health education initiatives on curbing typhoid fever outbreaks, particularly in resource-constrained regions. Nthiiri et al. [45] developed a mathematical model, comprising a set of ordinary differential equations, to analyze the dynamics of typhoid fever infection, considering resistance to infection. Adeboye et al. [13] formulated and explored a mathematical model addressing the co-infection of typhoid and malaria, aiming to control the spread of both diseases simultaneously. Pitzer et al. [46] investigated an age-structured mathematical model of typhoid fever to estimate the direct and indirect impacts of vaccination. Cook et al. [17] examined a mathematical model discussing the safety and efficacy of vaccination, both directly and indirectly, in the context of widespread vaccination programs.

Khan et al. [34] introduced a mathematical model and analysis of a deterministic framework that describes the transmission dynamics of typhoid fever. The model categorizes the total population $N(t)$ into four distinct compartments:

(i) $S(t)$: Describes dynamics of susceptible humans,
(ii) $E(t)$: Describes dynamics of unprotected humans,
(iii) $I(t)$: Describes dynamics of infected humans,
(iv) $R(t)$: Describes dynamics of recovered humans,

and the total population is expressed as $N(t) = S(t)+E(t)+I(t)+R(t)$. Using the SEIR model, Figure 1 illustrates a fractional map of the typhoid disease transmission between exposed individual compartments.

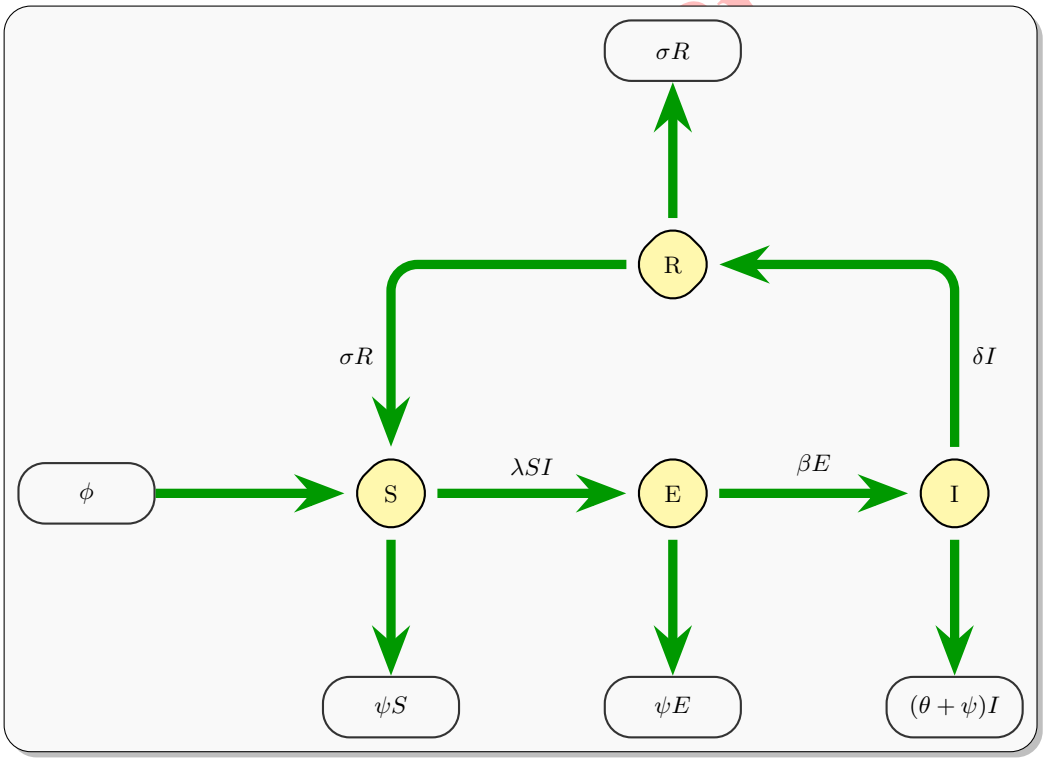

FIGURE 1. Diagrammatic representation of the epidemic model (Source: [34])

$$\frac{dS}{d\xi} = \phi + \sigma R - \lambda SI - \psi S, \tag{1.1}$$

$$\frac{dE}{d\xi} = \lambda SI - \beta E - \psi E, \tag{1.2}$$

$$\frac{dI}{d\xi} = \beta E - \theta I - \delta I - \psi I, \tag{1.3}$$

$$\frac{dR}{d\xi} = \delta I - \sigma R - \psi R. \tag{1.4}$$

TABLE 1. Description of Parameters

Parameter	Description
δ	The number of individuals succumbing to illness
λ	The rate at which diseases interact
ψ	The rate of natural mortality
β	The rate of symptomatic transmission
θ	The rate of recovery from infection
ϕ	The rate of human recruitment (birth)
σ	The rate of loss of temporary immunity in recovered individuals

Fractional calculus has emerged as a powerful mathematical tool due to its ability to capture memory effects and hereditary properties in dynamic systems, making it particularly effective for modeling complex biological and epidemiological phenomena [53, 55]. These systems are prevalent in various disciplines, including physics [28, 29], fluid mechanics, materials science, engineering [10, 11, 25], medical science [1, 3, 12, 36, 52], economics, and many others [4, 23, 43, 48]. Jalil and Mehrdad [37] derive exact periodic and solitary wave solutions of the integrable sixth-order Drinfeld–Sokolov–Satsuma–Hirota system by employing both the generalized (G'/G)-expansion and the generalized tanh–coth methods, showcasing their effectiveness for symbolic computation in nonlinear PDEs. Jalil et al. [38] present a systematic comparison between the generalized tanh–coth method and the (G'/G)-expansion method—applied to both nonlinear partial differential equations and ordinary differential equations—demonstrating that the tanh–coth method emerges as a specific case under the broader (G'/G)-expansion framework.

Integrated into mathematical modeling, fractional calculus provides a more accurate and flexible representation of real-world processes by incorporating nonlocality and time-dependent behavior [6, 21, 43]. This combination enables improved simulation, prediction, and analysis of system dynamics, and plays a vital role in formulating and assessing control strategies, especially in the context of disease transmission and intervention planning [20, 26, 35, 39]. Ibrahim et. al [32] introduced a theoretical and numerical analysis of a coronavirus (COVID-19) infection model based on a collection of fractional differential equations. Ahmed et. al [2] developed an accurate approximation of the fractional derivative with a non-singular kernel, and provide the numerical solution of the blood ethanol concentration system. Adel et al. [5] presented a numerical study for the blood ethanol concentration system (BECS) and the Lotka-Volterra system employing an accurate variational iteration method of development.

In recent years, mathematical modeling has become a cornerstone for analyzing and simulating complex systems across domains such as epidemiology, cyber security, and environmental science. Mohammed and Zaheer [41] introduced Neuro Cyber Guard, a deep neural learning-based framework that tightly integrates mathematical modeling with machine learning to construct robust defense mechanisms against cyber threats, effectively preserving system invariants during real-time operation. Alsalami [9] developed an Optimal Fully Connected Deep Neural Network (OFCDNN-SA) for sentiment analysis on social media, leveraging GloVe embeddings and salp swarm–optimized hyperparameters to support high-dimensional data interpretation by uncovering latent structures. Hussan et al. [31] designed a deep belief network for vulnerability detection in smart environments, adeptly capturing hidden system interactions consistent with dynamic modeling goals. Shakir [50] employed deep learning and remote sensing for smart sugarcane crop monitoring, showcasing the predictive power of modeling in precision agriculture. Additionally, Ahmed

and Mustafai [7] implemented convolutional neural networks optimized by Sea Lion Optimization for vehicle detection, illustrating how machine learning can address optimization challenges in mathematical models.

In this study, we analyzed fractional typhoid fever model using the homotopy decomposition method [24, 27], which provides a solution to the fractional differential equations by combining homotopy theory with the Cauchy n-order integral formula. In comparison with other methods, the homotopy decomposition method (HDM) does not require linearization or assumptions of weak nonlinearity. Unlike the Adomian decomposition method (ADM), it does not produce solutions in a general form, and does not involve Lagrange multipliers, which are essential in the variational iteration method (VIM). The proposed method also has limitations: the convergence of the series solution is not always guaranteed and can be slow for highly nonlinear or complex problems. The derived system is investigated through graphical simulations to assess the influence of key parameters on the transmission dynamics of the disease.

The rest of the article is organized as follows: section 2 provides fundamental definitions. Section 3 discusses the fractionalized model, equilibrium points, and their stability. Section 4 presents the solution of the proposed model. Section 5 examines the convergence analysis of the method. Section 6 includes numerical simulations and graphical discussions. Finally, we conclude our work in section 7. References are given at the end of the paper.

2. Fractional calculus

The Riemann-Liouville (RL) fractional derivative [15], notable for its independence from the continuity requirement at the origin and the condition of differentiability, serves as an extended form of Cauchy's integral, ranging from natural numbers to real numbers.

Definition 2.1. The RL fractional derivative of τ of order $\beta > 0$ is defined as follows [15, 47].

$$ {}_{a}^{RL}D_{\xi}^{\beta}\tau(\xi) = \frac{1}{\Gamma(q-\beta)}\frac{d^q}{d\xi^q}\int_a^{\xi}(\xi-\Psi)^{q-\beta-1}\tau(\Psi)\,d\Psi\,,\ \xi>0,\ q-1<\varsigma\le q,\ q\in Z^{+}. \tag{2.1} $$

Definition 2.2. A real-valued function $\tau(\xi)$, $\xi > 0$, is called in space C_{υ}, if $\exists$ a real number $\mathrm{K} > \upsilon$ such that $\tau(\xi) = \xi^{\mathrm{K}}\tau_1(\xi)$, where $\tau_1(\xi) \in C[0,\infty)$, and it is said to be in C_{υ}^{σ} if $\tau^{(\sigma)} \in C_{\upsilon}$, $\sigma \in N$.

Definition 2.3. The RL fractional integral of $\tau \in C_{\upsilon}$, $\upsilon \ge -1$ of order β, is defined as follows [15, 47].

$$ \Im^{\beta}[\tau(\xi)] = \frac{1}{\Gamma(\beta)}\int_0^{\xi}(\xi-\Psi)^{\beta-1}\tau(\Psi)d\Psi,\ \ \beta>0,\ \xi>0, \tag{2.2} $$

and

$$ \Im^{0}[\tau(\xi)] = \tau(\xi)\,. \tag{2.3} $$

3. The fractionalized model of typhoid fever disease

Since fractional models incorporate non-integer order derivatives, they account for memory and hereditary properties of the system, making them more suitable for accurately describing complex and history-dependent phenomena such as the spread of infectious diseases. Motivated by the advantages of fractional calculus, we reformulate the typhoid fever model (1.1)–(1.4) into a fractional-order system using the Riemann–Liouville fractional derivative operator.

$$ D_{\xi}^{\varsigma}S(\xi) = \phi + \sigma R - \lambda SI - \psi S, \tag{3.1} $$

$$ D_{\xi}^{\varsigma}E(\xi) = \lambda SI - \beta E - \psi E, \tag{3.2} $$

$$ D_{\xi}^{\varsigma}I(\xi) = \beta E - \theta I - \delta I - \psi I \tag{3.3} $$

$$D_{\xi}^{\varsigma} R(\xi) = \delta I - \sigma R - \psi R. \tag{3.4}$$

with initial conditions

$$S(0) = S_0,\ E(0) = E_0,\ I(0) = I_0,\ and\ R(0) = R_0. \tag{3.5}$$

Since we are dealing with a population model, all population compartments remain positive for all $\xi > 0$ within the feasible region $\Delta = \{S, E, I, R\} \in \Delta \subset \mathbb{R}_+^4$. It can be shown that all solutions are bounded in Δ for all $\xi > 0$, such that $0 \leq N \leq \frac{\phi}{\psi}$. This ensures that the model is epidemiologically well-posed within the region Δ and is therefore justified for further analysis.

3.1. **Equilibrium points.** To find the equilibrium of the typhoid fever model (3.1)-(3.4) with fractional derivatives in the sense of R-L derivative, we must set

$$\begin{aligned}
0 &= \phi + \sigma R - \lambda SI - \psi S,\\
0 &= \lambda SI - \beta E - \psi E,\\
0 &= \beta E - \theta I - \delta I - \psi I,\\
0 &= \delta I - \sigma R - \psi R.
\end{aligned}$$

Solving these equations, we get two equilibrium points:

1. Virus-free equilibrium (E_0)**:**

$$E_0 = \left(S^0,\ E^0,\ I^0,\ R^0\right) = \left(\frac{\phi}{\psi}, 0, 0, 0\right).$$

2. Endemic equilibrium (E_1)**:** $E^* = (S^*,\ E^*,\ I^*,\ R^*)$,
where,

$$\begin{aligned}
S^* &= \tfrac{(\beta+\psi)(\theta+\delta+\psi)}{\lambda\beta},\\
E^* &= \tfrac{(\theta+\delta+\psi)(\sigma+\psi)(\phi\beta\lambda-\psi(\beta+\psi)(\theta+\delta+\psi))}{\lambda\beta[(\sigma+\psi)(\beta+\psi)(\theta+\delta+\psi)]-\delta\beta\sigma},\\
I^* &= \tfrac{(\sigma+\psi)}{\alpha}\left(\tfrac{\phi\beta\lambda-\psi(\beta+\psi)(\theta+\delta+\psi)}{[(\sigma+\psi)(\beta+\psi)(\theta+\delta+\psi)]-\delta\beta\sigma}\right),\\
R^* &= \tfrac{1}{\alpha}\tfrac{[\phi\delta\beta\lambda-\delta\psi[(\beta+\psi)(\theta+\delta+\psi)]]}{((\sigma+\psi)(\beta+\psi)(\theta+\delta+\psi)-\delta\beta\sigma)}.
\end{aligned}$$

3.2. **Basic Reproductive Number.** , The basic reproductive number (R_0), which is the average number of secondary infections caused by an infectious individual introduced into a completely susceptible population, is obtained using the next generation matrix as indicated here using the infected compartment E and I, their rate of change equations and considering the partial derivatives of and with respect to E and I leading to square matrices and, respectively, described as

$$F = \begin{pmatrix} 0 & 0 \\ \lambda S & 0 \end{pmatrix}, \quad and \quad V = \begin{pmatrix} (\beta+\psi) & -\beta \\ 0 & (\theta+\delta+\psi) \end{pmatrix}.$$

Finding inverse of V and multiplying it with F

$$V^{-1} = \begin{pmatrix} \frac{1}{(\beta+\psi)} & \frac{\beta}{(\beta+\psi)(\theta+\delta+\psi)} \\ 0 & \frac{1}{(\theta+\delta+\psi)} \end{pmatrix},$$

$$FV^{-1} = \begin{pmatrix} 0 & 0 \\ \frac{\lambda S}{(\beta+\psi)} & \frac{\beta\lambda S}{(\beta+\psi)(\theta+\delta+\psi)} \end{pmatrix}.$$

Introducing Eigen values and solving the determinant gives two Eigen values as follows $\lambda_1 = 0$ and $\lambda_1 = \frac{\beta\lambda S}{(\beta+\psi)(\theta+\delta+\psi)}$. The most dominant eigenvalue is $\lambda_1 = 0$ and $\lambda_1 = \frac{\beta\lambda S}{(\beta+\psi)(\theta+\delta+\psi)}$ which forms our basic reproductive number. At

disease free equilibrium $R_0 = \frac{\beta\lambda\phi}{\psi(\beta+\psi)(\theta+\delta+\psi)}$.

Theorem 3.1. *Disease free equilibrium is locally asymptotically stable if less than unity and unstable if greater than unity.*

Proof. Basic reproductive number is

$$R_0 = \frac{\beta\lambda\phi}{\psi\left(\beta+\psi\right)\left(\theta+\delta+\psi\right)}.$$

At Disease Free Equilibrium $R_0 < 1$, hence

$$\frac{\beta\lambda\phi}{\psi\left(\beta+\psi\right)\left(\theta+\delta+\psi\right)} < 1,$$

or,

$$\beta < \frac{\psi^2\left(\theta+\delta+\psi\right)}{\lambda\phi-\psi\left(\theta+\delta+\psi\right)}.$$

Therefore, if $\beta < \frac{\psi^2(\theta+\delta+\psi)}{\lambda\phi-\psi(\theta+\delta+\psi)}$, disease free equilibrium will be locally stable.
Similarly, if $R_0 > 1$, then it follows that

$$\frac{\beta\lambda\phi}{\psi\left(\beta+\psi\right)\left(\theta+\delta+\psi\right)} > 1.$$

This implies that

$$\beta > \frac{\psi^2\left(\theta+\delta+\psi\right)}{\lambda\phi-\psi\left(\theta+\delta+\psi\right)},$$

which means that disease free equilibrium is locally asymptotically unstable.

□

4. Proposed Methodology

Let's examine a fractional-order non-homogeneous differential equation represented as follows [25, 30].

$$D_{\xi}^{\beta}\left[\tau\left(\xi\right)\right] = \Re\left[\tau\left(\xi\right)\right] + \aleph\left[\tau\left(\xi\right)\right] + h\left(\xi\right), \quad 0 < \beta \leq 1, \tag{4.1}$$

accompanied by the initial condition:

$$\tau\left(\xi_0\right) = \varphi, \tag{4.2}$$

where, D_{ξ}^{β} denotes RL derivative with fractional order β, $\Re$ and $\aleph$ represent linear and nonlinear functions, respectively, while h is source term. In this way, first, we transform the fractional differential equation to the fractional integral equation

$$\tau\left(\xi\right) - \tau\left(0\right) = \frac{1}{\Gamma\beta}\int_{0}^{\xi}\left(\xi-\mu\right)^{\beta-1}\left[\Re\left[\tau\left(\mu\right)\right] + \aleph\left[\tau\left(\mu\right)\right] + h\left(\mu\right)\right]d\mu\,. \tag{4.3}$$

According to the given approach, the solution may be written as the following power series:

$$\tau\left(\xi,p\right) = \sum_{\varrho=0}^{\infty} p^{\varrho}\tau_{\varrho}\left(\xi\right), \tag{4.4}$$

and

$$\tau\left(\xi\right) = \lim_{p\to 1}\tau\left(\xi,p\right). \tag{4.5}$$

While, the nonlinear term $\aleph[\tau(\xi)]$ is decomposed as

$$\aleph[\tau(\xi)] = \sum_{\varrho=0}^{\infty} p^{\varrho} H_{\varrho}(\tau), \tag{4.6}$$

where $p \in (0,1]$ denotes the embedding parameter. $H_{\varrho}(\tau)$ signifies He's polynomial, which can be stated as [8, 22, 51].

$$H_{\varrho}(\tau_0, \tau_1, \tau_2, ..., \tau_{\varrho}) = \frac{1}{\Gamma(\varrho+1)} \frac{\partial^{\varrho}}{\partial p^{\varrho}} \left[\aleph \left(\sum_{k=0}^{\infty} p^k \tau_k(\xi) \right) \right], \quad \rho = 0, 1, 2, ... \tag{4.7}$$

Replacing equations (4.4), (4.6), and (4.7) into equation (4.3), we get

$$\sum_{\varrho=0}^{\infty} p^{\varrho} \tau_{\varrho}(\xi) - \tau(0) = p \left(\frac{1}{\Gamma\beta} \int_0^{\xi} (\xi-\mu)^{\beta-1} \left[\Re \left[\sum_{\varrho=0}^{\infty} p^{\varrho} \tau_{\varrho}(\mu) \right] + \aleph \left[\sum_{\varrho=0}^{\infty} p^{\varrho} \tau_{\varrho}(\mu) \right] + h(\mu) \right] d\mu \right). \tag{4.8}$$

By comparing the identical powers of p on both sides, we find solutions of various orders, leading with an initial approximation

$$\tau_0(\xi) = \varphi. \tag{4.9}$$

In this paper, we modified the beta derivative for the first time, then Equation (4.1) becomes

$$\sum_{\varrho=0}^{\infty} p^{\varrho} \tau_{\varrho}(\xi) - \tau(0) = p \left(\frac{1}{\Gamma\beta} \int_0^{\xi} (\xi-\mu)^{\beta-1} \left[\Re \left[\sum_{\varrho=0}^{\infty} p^{\varrho} \tau_{\varrho}(\mu) \right] + \aleph \left[\sum_{\varrho=0}^{\infty} p^{\varrho} \tau_{\varrho}(\mu) \right] + h(\mu) \right] d\mu \right). \tag{4.10}$$

Thus, the solution of Equation (4.1) is given as

$$\tau = \tau_0 + \tau_1 + \tau_2 + ... + \tau_{\varrho}. \tag{4.11}$$

5. Stability Analysis of Proposed Model

Theorem 5.1. *Define Φ_1, Φ_2, Φ_3, and Φ_4, as well as their relationships to unknown variables.*

Proof. Firstly, we reduce Equations (3.1), (3.2), (3.3), and (3.4) into integral equations, respectively.

$$S(\xi) = S(0) + \frac{1}{\Gamma\varsigma} \int_0^{\xi} (\xi-\mu)^{\varsigma-1} [\phi + \sigma R(\mu) - \lambda S(\mu) I(\mu) - \psi S(\mu)] d\mu, \tag{5.1}$$

$$E(\xi) = E(0) + \frac{1}{\Gamma\varsigma} \int_0^{\xi} (\xi-\mu)^{\varsigma-1} [\lambda S(\mu) I(\mu) - \beta E(\mu) - \psi E(\mu)] d\mu, \tag{5.2}$$

$$I(\xi) = I(0) + \frac{1}{\Gamma\varsigma} \int_0^{\xi} (\xi-\mu)^{\varsigma-1} [\beta E(\mu) - \theta I(\mu) - \delta I(\mu) - \psi I(\mu)] d\mu, \tag{5.3}$$

$$R(\xi) = R(0) + \frac{1}{\Gamma\varsigma} \int_0^{\xi} (\xi-\mu)^{\varsigma-1} [\delta I(\mu) - \sigma R(\mu) - \psi R(\mu)] d\mu, \ 0 < \varsigma \leq 1, \tag{5.4}$$

here, we have the following kernels:

$$\Phi_1(\xi, S) = \phi + \sigma R(\xi) - \lambda S(\xi) I(\xi) - \psi S(\xi), \tag{5.5}$$

$$\Phi_2(\xi, E) = \lambda S(\xi) I(\xi) - \beta E(\xi) - \psi E(\xi), \tag{5.6}$$

$$\Phi_3(\xi, I) = \beta E(\xi) - \theta I(\xi) - \delta I(\xi) - \psi I(\xi), \tag{5.7}$$

$$\Phi_4(\xi, R) = \delta I(\xi) - \sigma R(\xi) - \psi R(\xi)\,. \tag{5.8}$$

□

Theorem 5.2. *Φ_1, Φ_2, and Φ_3 satisfy the Lipchitz condition.*

Proof. Firstly, we show that Φ_1 satisfies the Lipchitz condition. Let S and S_1 be two functions, then

$$\|\Phi_1(\xi, S) - \Phi_1(\xi, S_1)\| = \|(\phi + \sigma R(\xi) - \lambda S(\xi) I(\xi) - \psi S(\xi)) - (\phi + \sigma R(\xi) - \lambda S_1(\xi) I(\xi) - \psi S_1(\xi))\|\,, \tag{5.9}$$

using Cauchy's inequality, we have

$$\|\Phi_1(\xi, S) - \Phi_1(\xi, S_1)\| \leq \|\psi + \lambda I(\xi)\| \, \|S(\xi) - S_1(\xi)\|\,, \tag{5.10}$$

or

$$\|\Phi_1(\xi, S) - \Phi_1(\xi, S_1)\| \leq \Theta \, \|S(\xi) - S_1(\xi)\|\,, \tag{5.11}$$

where,

$$\|\psi + \lambda I(\xi)\| \leq \Theta. \tag{5.12}$$

Also for Φ_2

$$\|\Phi_2(\xi, E) - \Phi_2(\xi, E_1)\| = \|(\lambda S(\xi) I(\xi) - \beta E(\xi) - \psi E(\xi)) - (\lambda S(\xi) I(\xi) - \beta E_1(\xi) - \psi E_1(\xi))\|\,, \tag{5.13}$$

by using Cauchy's inequality, we have

$$\|\Phi_2(\xi, E) - \Phi_2(\xi, E_1)\| \leq \|(\beta + \psi)\| \, \|E(\xi) - E_1(\xi)\|\,, \tag{5.14}$$

or

$$\|\Phi_2(\xi, E) - \Phi_2(\xi, E_1)\| \leq \mu \, \|E(\xi) - E_1(\xi)\|\,, \tag{5.15}$$

where,

$$\|(\beta + \psi)\| \leq \mu. \tag{5.16}$$

Also for Φ_3

$$\|\Phi_3(\xi, I) - \Phi_3(\xi, I_1)\| = \|(\beta E(\xi) - \theta I(\xi) - \delta I(\xi) - \psi I(\xi)) - (\beta E(\xi) - \theta I_1(\xi) - \delta I_1(\xi) - \psi I_1(\xi))\|\,, \tag{5.17}$$

by using Cauchy's inequality, we have

$$\|\Phi_3(\xi, I) - \Phi_3(\xi, I_1)\| \leq \Omega \, \|I(\xi) - I_1(\xi)\|\,, \tag{5.18}$$

where,

$$\|\theta + \delta + \psi\| \leq \Omega\,. \tag{5.19}$$

Also for Φ_4

$$\|\Phi_4(\xi, R) - \Phi_4(\xi, R_1)\| = \|(\delta I(\xi) - \sigma R(\xi) - \psi R(\xi)) - (\delta I(\xi) - \sigma R_1(\xi) - \psi R_1(\xi))\|\,, \tag{5.20}$$

by using Cauchy's inequality, we have

$$\|\Phi_4(\xi, R) - \Phi_4(\xi, R_1)\| \leq \kappa \, \|R(\xi) - R_1(\xi)\|\,, \tag{5.21}$$

where,

$$\|\sigma + \psi\| \leq \kappa\,. \tag{5.22}$$

We take the recursive formula

$$S_{\varrho}(\xi) = \Phi_1(\xi, S_{\varrho-1}) + \frac{1}{\Gamma\varsigma}\int_0^{\xi}(\xi-\mu)^{\varsigma-1}\Phi_1(\mu, S_{\varrho-1})\,d\mu\,. \tag{5.23}$$

Now analyse the sequential difference of two terms

$$\begin{aligned} U_{\varrho}(\xi) &= S_{\varrho}(\xi) - S_{\varrho-1}(\xi) = \Phi_1(\xi, S_{\varrho-1}) - \Phi_1(\xi, S_{\varrho-2}) \\ &+\tfrac{1}{\Gamma\varsigma}\int_0^{\xi}(\xi-\mu)^{\varsigma-1}\left(\Phi_1(\mu, S_{\varrho-1}) - \Phi_1(\mu, S_{\varrho-2})\right)d\mu\,, \end{aligned} \tag{5.24}$$

by taking norm of Eq. (5.24), we have

$$\begin{aligned} \|U_{\varrho}(\xi)\| &= \|S_{\varrho}(\xi) - S_{\varrho-1}(\xi)\| \\ &= \left\| \begin{array}{l} \Phi_1(\xi, S_{\varrho-1}) - \Phi_1(\xi, S_{\varrho-2}) \\ +\tfrac{1}{\Gamma\varsigma}\int_0^{\xi}(\xi-\mu)^{\varsigma-1}\left(\Phi_1(\mu, S_{\varrho-1}) - \Phi_1(\mu, S_{\varrho-2})\right)d\mu \end{array} \right\|, \\ &\le \|\Phi_1(\xi, S_{\varrho-1}) - \Phi_1(\xi, S_{\varrho-2})\| \\ &+ \frac{1}{\Gamma\varsigma}\int_0^{\xi}\left\|(\xi-\mu)^{\varsigma-1}\left(\Phi_1(\mu, S_{\varrho-1}) - \Phi_1(\mu, S_{\varrho-2})\right)\right\|d\mu \end{aligned} \tag{5.25}$$

and similarly, we obtain

$$\begin{aligned} \|V_{\varrho}(\xi)\| &= \|E_{\varrho}(\xi) - E_{\varrho-1}(\xi)\| \\ &\le \|\Phi_2(\xi, E_{\varrho-1}) - \Phi_2(\xi, E_{\varrho-2})\| \\ &+ \frac{1}{\Gamma\varsigma}\int_0^{\xi}\left\|(\xi-\mu)^{\varsigma-1}\left(\Phi_2(\mu, E_{\varrho-1}) - \Phi_2(\mu, E_{\varrho-2})\right)\right\|d\mu\,, \end{aligned} \tag{5.26}$$

$$\begin{aligned} \|W_{\varrho}(\xi)\| &= \|I_{\varrho}(\xi) - I_{\varrho-1}(\xi)\| \\ &\le \|\Phi_3(\xi, I_{\varrho-1}) - \Phi_3(\xi, I_{\varrho-2})\| \\ &+ \frac{1}{\Gamma\varsigma}\int_0^{\xi}\left\|(\xi-\mu)^{\varsigma-1}\left(\Phi_3(\mu, I_{\varrho-1}) - \Phi_3(\mu, I_{\varrho-2})\right)\right\|d\mu\,, \end{aligned} \tag{5.27}$$

$$\begin{aligned} \|P_{\varrho}(\xi)\| &= \|R_{\varrho}(\xi) - R_{\varrho-1}(\xi)\| \\ &\le \|\Phi_4(\xi, R_{\varrho-1}) - \Phi_4(\xi, R_{\varrho-2})\| \\ &+ \frac{1}{\Gamma\varsigma}\int_0^{\xi}\left\|(\xi-\mu)^{\varsigma-1}\left(\Phi_4(\mu, R_{\varrho-1}) - \Phi_4(\mu, R_{\varrho-2})\right)\right\|d\mu\,. \end{aligned} \tag{5.28}$$

□

Theorem 5.3. *The fractional typhoid fever model has a solution, under the restriction with* ξ_0 *as* $\Im_1 + J_1(\xi_0)^{\varsigma} < 1$, $\Im_2 + J_2(\xi_0)^{\varsigma} < 1$, *and* $\Im_3 + J_3(\xi_0)^{\varsigma} < 1$.

Proof. Since Eqs. (5.25), (5.26), (5.27), and (5.28) are bounded and the kernels Φ_1, Φ_2, Φ_3, and Φ_4 satisfy the Lipchitz conditions. As a result of the outcomes of the recursive technique, we have

$$\|U_{\varrho}(\xi)\| \le \|S(0)\|\{\Im_1 + J_1(\xi_0)^{\varsigma}\}^{\varrho}. \tag{5.29}$$

As a result, the aforementioned results are both continuous and present. Furthermore, to show that solutions of Eq. (3.1) as described before, we have

$$S(\xi) - S(0) = S_{\varrho}(\xi) - \wp_{\varrho}(\xi), \tag{5.30}$$

thus, we have

$$\|\wp_{\varrho}(\xi)\| = \left\| \begin{array}{l} (\Phi_1(\xi, S) - \Phi_1(\xi, S_{\varrho-1}))\, x \\ +\frac{1}{\Gamma\varsigma} \int_0^{\xi} (\xi-\mu)^{\varsigma-1} (\Phi_1(\mu, S) - \Phi_1(\mu, S_{\varrho-1}))\, d\mu \end{array} \right\|, \tag{5.31}$$

or

$$\begin{aligned} \|\wp_{\varrho}(\xi)\| &\leq \|(\Phi_1(\xi, S) - \Phi_1(\xi, S_{\varrho-1}))\| \\ &\quad + \frac{1}{\Gamma\varsigma} \left\| \int_0^{\xi} (\xi-\mu)^{\varsigma-1} (\Phi_1(\mu, S) - \Phi_1(\mu, S_{\varrho-1})) \right\| d\mu, \end{aligned} \tag{5.32}$$

or

$$\|\wp_{\varrho}(\xi)\| \leq \Im \|S - S_{\varrho-1}\| + \xi^{\varsigma} J \|S - S_{\varrho-1}\|, \tag{5.33}$$

by recursively solving, we obtain

$$\|\wp_{\varrho}(\xi)\| \leq \{\Im_1 + J_1 \xi^{\varsigma}\}^{\varrho+1} \Psi, \tag{5.34}$$

thus at ξ_0

$$\|\wp_{\varrho}(\xi)\| \leq \{\Im_1 + J_1 \xi_0^{\varsigma}\}^{\varrho+1} \Psi, \tag{5.35}$$

as $\lim \varrho \to \infty$, we have

$$\|\wp_{\varrho}(\xi)\| \to 0. \tag{5.36}$$

Thus, we have proven the existence and can establish further findings in the same way. □

Theorem 5.4. *The fractional typhoid fever model possesses a unique solution.*

Proof. To demonstrate the uniqueness, we suppose that there is another set of solutions for the system (3.1), (3.2), (3.3), and (3.4) which are provided by $S(\xi)$, $E(\xi)$, $I(\xi)$, and $R(\xi)$. Firstly, we consider

$$\begin{aligned} S(\xi) - S_1(\xi) &= (\Phi_1(\xi, S) - \Phi_1(\xi, S_1)) \\ &\quad + \frac{1}{\Gamma\varsigma} \int_0^{\xi} (\xi-\mu)^{\varsigma-1} (\Phi_1(\mu, S) - \Phi_1(\mu, S_1))\, d\mu, \end{aligned} \tag{5.37}$$

taking the norm of Eq. (5.37), we obtain

$$\begin{aligned} \|S(\xi) - S_1(\xi)\| &\leq \|(\Phi_1(\xi, S) - \Phi_1(\xi, S_1))\| \\ &\quad + \frac{1}{\Gamma\varsigma} \int_0^{\xi} \left\| \left\{ (\xi-\mu)^{\varsigma-1} (\Phi_1(\mu, S) - \Phi_1(\mu, S_1)) \right\} \right\| d\mu. \end{aligned} \tag{5.38}$$

Since the solution is bounded, the Lipchitz condition provides.

$$S(\xi) = S_1(\xi). \tag{5.39}$$

Similarly, we obtain

$$E(\xi) = E_1(\xi), \tag{5.40}$$

and

$$I(\xi) = I_1(\xi). \tag{5.41}$$

Hence, we conclude that the model has unique solution. □

6. Approximate solution of typhoid fever model

According to suggested technique, we have

$$\sum_{\varrho=0}^{\infty} p^{\varrho} S_{\varrho}(\xi) = S(0) + \frac{p}{\Gamma\varsigma} \int_0^{\xi} (\xi-\mu)^{\varsigma-1} \left[\phi + \sigma \left(\sum_{\varrho=0}^{\infty} p^{\varrho} R_{\varrho}(\mu) \right) - \lambda \left(\sum_{\varrho=0}^{\infty} p^{\varrho} S_{\varrho}(\mu) \sum_{\varrho=0}^{\infty} p^{\varrho} I_{\varrho}(\mu) \right) - \psi \left(\sum_{\varrho=0}^{\infty} p^{\varrho} S_{\varrho}(\mu) \right) \right] d\mu, \tag{6.1}$$

$$\sum_{\varrho=0}^{\infty} p^{\varrho} E_{\varrho}(\xi) = E(0) + \frac{p}{\Gamma\varsigma} \int_0^{\xi} (\xi-\mu)^{\varsigma-1} \left[\lambda \left(\sum_{\varrho=0}^{\infty} p^{\varrho} S_{\varrho}(\mu) \sum_{\varrho=0}^{\infty} p^{\varrho} I_{\varrho}(\mu) \right) - (\beta+\psi) \left(\sum_{\varrho=0}^{\infty} p^{\varrho} E_{\varrho}(\mu) \right) \right] d\mu, \tag{6.2}$$

$$\sum_{\varrho=0}^{\infty} p^{\varrho} I_{\varrho}(\xi) = I(0) + \frac{p}{\Gamma\varsigma} \int_0^{\xi} (\xi-\mu)^{\varsigma-1} \left[\beta \left(\sum_{\varrho=0}^{\infty} p^{\varrho} E_{\varrho}(\mu) \right) - (\theta+\delta+\psi) \left(\sum_{\varrho=0}^{\infty} p^{\varrho} I_{\varrho}(\mu) \right) \right] d\mu, \tag{6.3}$$

and

$$\sum_{\varrho=0}^{\infty} p^{\varrho} R_{\varrho}(\xi) = R(0) + \frac{p}{\Gamma\varsigma} \int_0^{\xi} (\xi-\mu)^{\varsigma-1} \left[\delta \left(\sum_{\varrho=0}^{\infty} p^{\varrho} I_{\varrho}(\mu) \right) - (\sigma+\psi) \left(\sum_{\varrho=0}^{\infty} p^{\varrho} R_{\varrho}(\mu) \right) \right] d\mu. \tag{6.4}$$

Computing the coefficients of different powers of p on both sides, we get

$$p^0 : S_0(\xi) = S(0), \qquad S(0) = S_0, \tag{6.5}$$

$$p^0 : E_0(\xi) = E(0), \qquad E(0) = E_0, \tag{6.6}$$

$$p^0 : I_0(\xi) = I(0), \qquad I(0) = I_0, \tag{6.7}$$

and

$$p^0 : R_0(\xi) = R(0), \qquad R(0) = R_0 . \tag{6.8}$$

Also,

$$p^1 : S_1(\xi) = \frac{1}{\Gamma\varsigma} \int_0^{\xi} (\xi-\mu)^{\varsigma-1} [\phi + \sigma R_0(\mu) - \lambda S_0(\mu) I_0(\mu) - \psi S_0(\mu)] d\mu, \tag{6.9}$$

$$p^1 : E_1(\xi) = \frac{1}{\Gamma\varsigma} \int_0^{\xi} (\xi-\mu)^{\varsigma-1} [\lambda S_0(\mu) I_0(\mu) - (\beta+\psi) E_0(\mu)] d\mu, \tag{6.10}$$

$$p^1 : I_1(\xi) = \frac{1}{\Gamma\varsigma} \int_0^{\xi} (\xi-\mu)^{\varsigma-1} [\beta E_0(\mu) - (\theta+\delta+\psi) I_0(\mu)] d\mu, \tag{6.11}$$

$$p^1 : R_1(\xi) = \frac{1}{\Gamma\varsigma}\int_0^{\xi}(\xi-\mu)^{\varsigma-1}[\delta I_0(\mu) - (\sigma+\psi)R_0(\mu)]d\mu, \tag{6.12}$$

in the same manner

$$p^2 : S_2(\xi) = \frac{1}{\Gamma\varsigma}\int_0^{\xi}(\xi-\mu)^{\varsigma-1}[\phi + \sigma R_1(\mu) - \lambda S_0(\mu)I_1(\mu) \ -\lambda S_1(\mu)I_0(\mu) - \psi S_1(\mu)]\,d\mu, \tag{6.13}$$

$$p^2 : E_2(\xi) = \frac{1}{\Gamma\varsigma}\int_0^{\xi}(\xi-\mu)^{\varsigma-1}[\lambda(S_0(\mu)I_1(\mu)) + \lambda(S_1(\mu)I_0(\mu)) \ -(\beta+\psi)E_1(\mu)]\,d\mu, \tag{6.14}$$

$$p^2 : I_2(\xi) = \frac{1}{\Gamma\varsigma}\int_0^{\xi}(\xi-\mu)^{\varsigma-1}[\beta E_1(\mu) - (\theta+\delta+\psi)I_1(\mu)]d\mu, \tag{6.15}$$

$$p^2 : R_2(\xi) = \frac{1}{\Gamma\varsigma}\int_0^{\xi}(\xi-\mu)^{\varsigma-1}[\delta I_1(\mu) - (\sigma+\psi)R_1(\mu)]d\mu, \tag{6.16}$$

$$\vdots$$

$$p^{\varrho} : S_{\varrho}(\xi) = \frac{1}{\Gamma\varsigma}\int_0^{\xi}(\xi-\mu)^{\varsigma-1}\left[\phi + \sigma R_{\varrho-1}(\mu) - \lambda\sum_{j=0}^{\varrho-1}(S_j(\mu)I_{\varrho-j-1}(\mu)) - \psi S_{\varrho-1}(\mu)\right]d\mu, \tag{6.17}$$

$$p^{\varrho} : E_{\varrho}(\xi) = \frac{1}{\Gamma\varsigma}\int_0^{\xi}(\xi-\mu)^{\varsigma-1}\left[\lambda\sum_{j=0}^{\varrho-1}(S_j(\mu)I_{\varrho-j-1}(\mu)) - (\beta+\psi)E_{\varrho-1}(\mu)\right]d\mu, \tag{6.18}$$

$$p^{\varrho} : I_{\varrho}(\xi) = \frac{1}{\Gamma\varsigma}\int_0^{\xi}(\xi-\mu)^{\varsigma-1}[\beta E_{\varrho-1}(\mu) - (\theta+\delta+\psi)I_{\varrho-1}(\mu)]d\mu, \tag{6.19}$$

$$p^{\varrho} : R_{\varrho}(\xi) = \frac{1}{\Gamma\varsigma}\int_0^{\xi}(\xi-\mu)^{\varsigma-1}[\delta I_{\varrho-1}(\mu) - (\sigma+\psi)R_{\varrho-1}(\mu)]d\mu, \tag{6.20}$$

hence, the solution of proposed model is given as

$$S(\xi) = S_0 + S_1(\xi) + S_2(\xi) + \ldots\ldots\ldots \tag{6.21}$$

$$E(\xi) = E_0 + E_1(\xi) + E_2(\xi) + \ldots\ldots \tag{6.22}$$

$$I(\xi) = I_0 + I_1(\xi) + I_2(\xi) + \ldots\ldots\ldots \tag{6.23}$$

$$R(\xi) = R_0 + R_1(\xi) + R_2(\xi) + \ldots\ldots\ldots \tag{6.24}$$

7. Results and discussions

This section presents the numerical results and analytical behavior of the proposed fractional-order typhoid fever model, solved using the homotopy decomposition method (HDM). The model incorporates the Riemann–Liouville fractional derivative and accounts for memory effects that are essential in disease dynamics. All simulations are based on the following parameter values: $\varphi = 0.75, \beta = 1.99, \psi = 0.02, \theta = 0.1503, \lambda = 0.0125, \delta = 0.625$, and $\sigma = 0.125$, as referenced in prior studies [34]. Figures 2(a), 3(a), 4(a), and 5(a) illustrate the temporal evolution of the susceptible $S(\xi)$, exposed $E(\xi)$, infected $I(\xi)$, and recovered $R(\xi)$ populations for varying fractional orders $\zeta \in \{0.8, 0.85, 0.9, 0.95, 1\}$. In Figure 2(a), the number of exposed individuals increases as the fractional order approaches one, indicating that the disease model behaves more like traditional integer-order dynamics. Figure 3(a) shows that vaccination consistently reduces the number of infected individuals, with this effect being more pronounced at lower fractional orders, where memory effects are stronger. In Figure 4(a), the recovered population grows over time in all cases, but the rate and stabilization point differ. Lower fractional orders result in slower recoveries and longer stabilization times, while higher orders lead to faster recovery rates. Figure 5(a) demonstrates that the total number of cases remains significantly lower when memory effects are more prominent. Collectively, these figures highlight that models incorporating stronger memory effects not only reduce the number of infections but also enhance the effectiveness of vaccination, underscoring the power of fractional calculus in understanding and controlling disease spread.

Figures 2(c), 3(c), 4(c), and 5(c)show the impact of varying the transmission rate β on model dynamics. For increasing values of $\beta \in \{0.0199, 0.199, 1.99\}$, there is a notable rise in the exposed $E(\xi)$ and infected $I(\xi)$ populations, along with a faster decline in the susceptible $S(\xi)$ class. These results confirm that the transmission rate is directly proportional to disease spread. As β increases, the infection becomes more aggressive, leading to a sharper rise in prevalence and faster growth in the recovered population due to the higher turnover of infected individuals. This sensitivity to β highlights the importance of interventions such as vaccination, public health campaigns, or isolation strategies in reducing effective transmission. Figures 2(d), 3(d), 4(d), and 5(d) show that a higher infection interaction rate λ intensifies contact-based transmission, causing the exposed and infected populations to peak earlier and at higher levels. Consequently, the susceptible population declines more rapidly, while the recovered population grows at an accelerated rate.

Figures 2(e), 3(e), 4(e), and 5(e) demonstrate that increasing the recovery rate θ leads to a lower peak and shorter duration for the infected compartment $I(\xi)$, while accelerating the growth of the recovered compartment $R(\xi)$. This increase in θ also slows the depletion of the susceptible class $S(\xi)$, as fewer infectious individuals are available to drive new infections. These dynamics indicate that higher values of θ, whether due to improved healthcare or enhanced natural immunity, effectively reduce the infection burden and assist in epidemic control.

Figures 2(f), 3(f), 4(f), and 5(f) assess the influence of the natural mortality rate ψ. As ψ increases, all compartments display reduced values over time, reflecting the background attrition of the population due to natural death. Further, We compared the solution obtained by the proposed method (using up to ten terms) with that of the classical RK-4 method for the integer-order case, as shown in Figures 2(b), 3(b), 4(b), and 5(b). These figures demonstrate that the solutions from both methods are in close agreement, validating the homotopy decomposition method as a robust and accurate semi-analytical tool for solving fractional epidemiological models, even in the presence of nonlinear and complex system behavior.

Finally, the traveling wave solutions obtained from our fractional-order model exhibit realistic epidemic wave structures characterized by sharp onset, pronounced peaks, and gradual declines. The fractional order serves as a memory parameter lower values delay and flatten the peak, reflecting slower immune or behavioral responses. The model provides explicit expressions for wavefront propagation speed and peak infection magnitude, allowing quantitative forecasting of outbreak timing and intensity based on fractional dynamics. These analytical insights can inform timely vaccination campaigns or sanitation measures before peak incidence, thereby enhancing the practical utility of fractional epidemiological modeling.

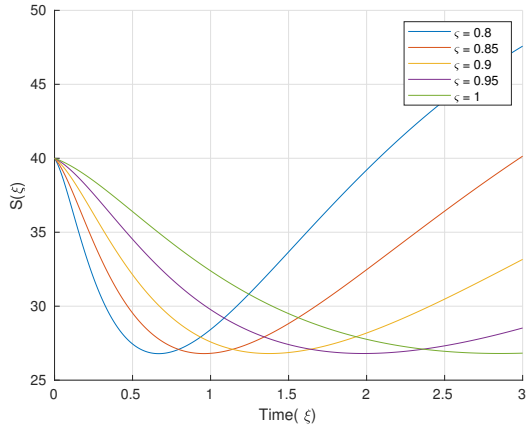

(a) Graphical representation of susceptible individuals corresponding to different fractional order of the proposed model.

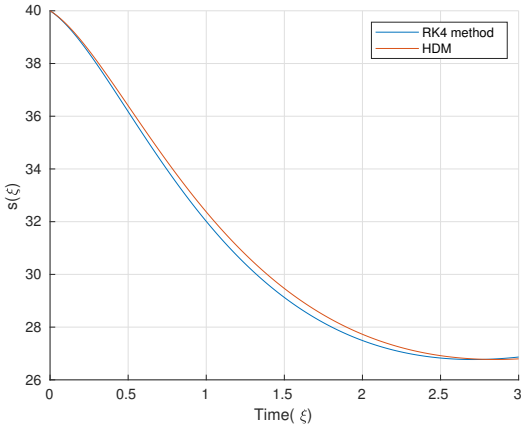

(b) Comparison between our proposed solution up to ten terms with that of RK4 method for susceptible individuals of the proposed model.

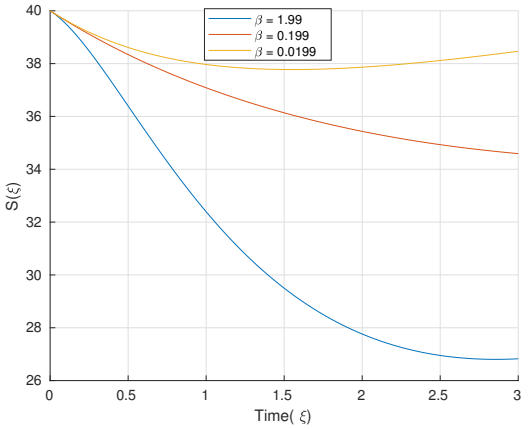

(c) Suspected cases rate for different values of β.

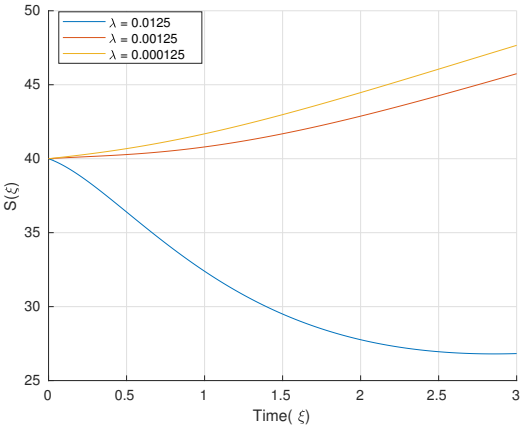

(d) Suspected cases rate for different values of λ.

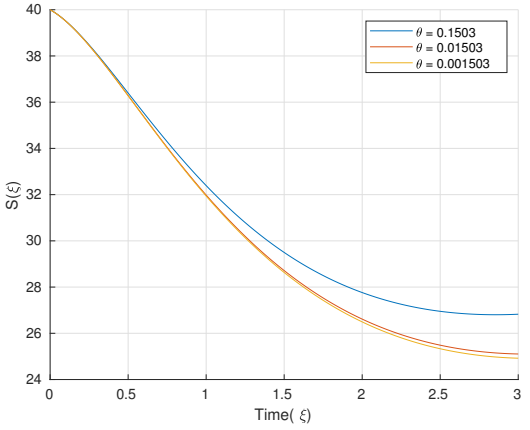

(e) Suspected cases rate for different values of θ.

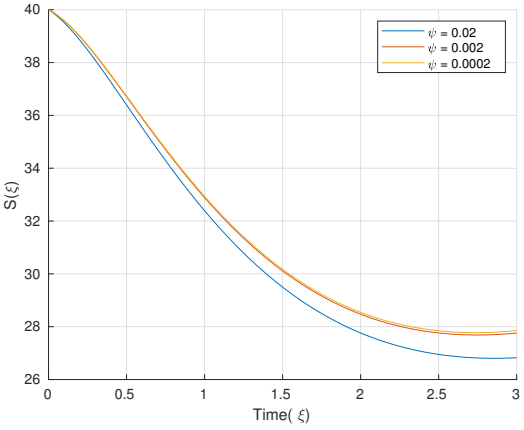

(f) Suspected cases rate for different values of ψ.

FIGURE 2. 2-D behviour of suspected population for various parameters.

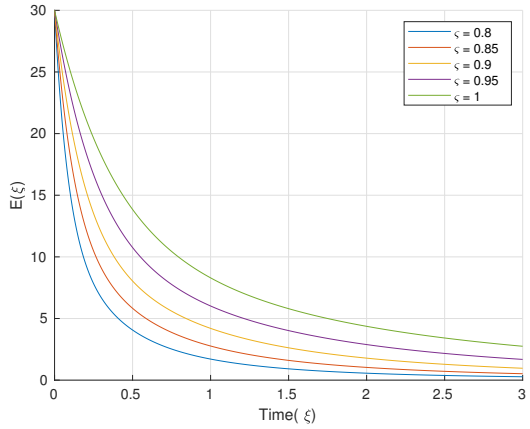

(a) Graphical representation of exposed individuals corresponding to different fractional order of the proposed model.

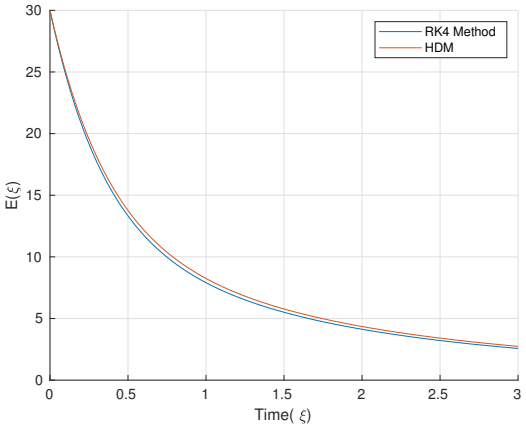

(b) Comparison between our proposed solution up to ten terms with that of RK4 method for exposed individuals of the proposed model.

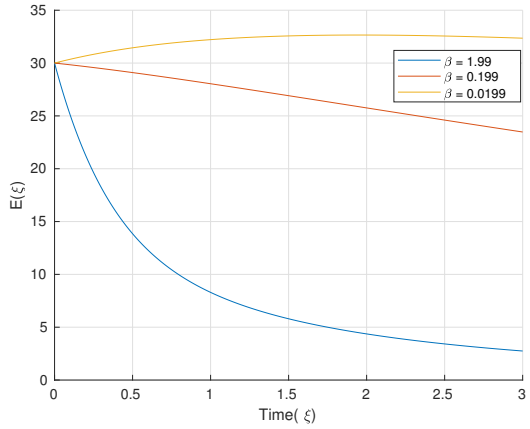

(c) Exposed cases rate for different values of β.

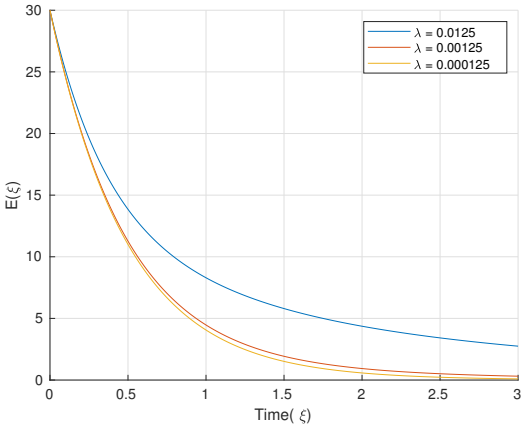

(d) Exposed cases rate for different values of λ.

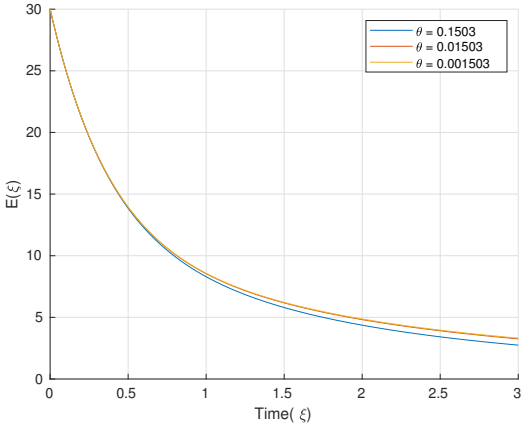

(e) Exposed cases rate for different values of θ.

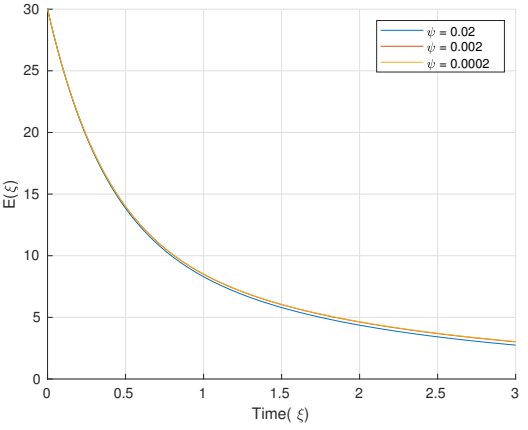

(f) Exposed cases rate for different values of ψ.

FIGURE 3. 2-D behviour of Exposed population for various parameters.

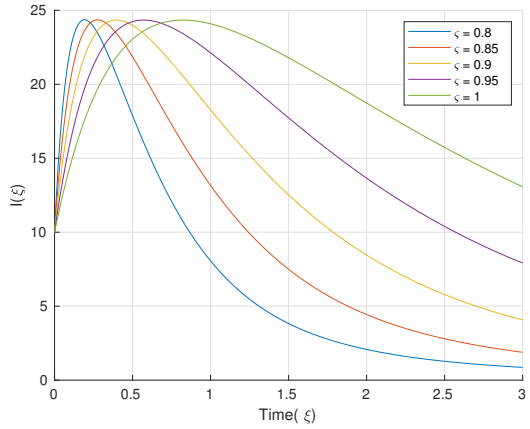

(a) Graphical representation of infected individuals corresponding to different fractional order of the proposed model.

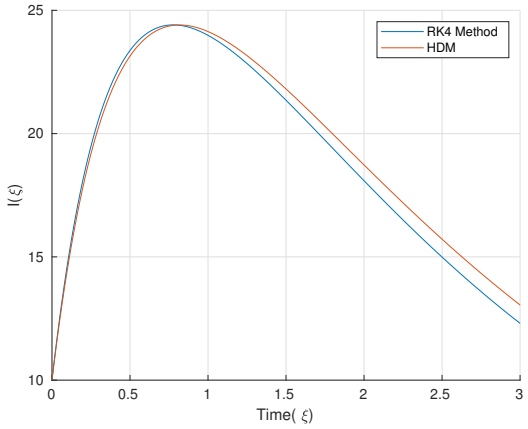

(b) Comparison between our proposed solution up to ten terms with that of RK4 method for infected individuals of the proposed model.

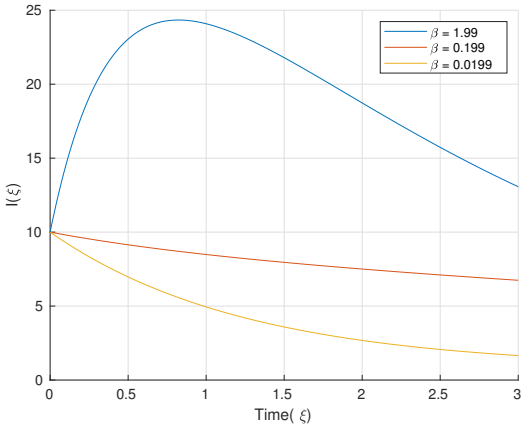

(c) Infected individuals cases rate for different values of β.

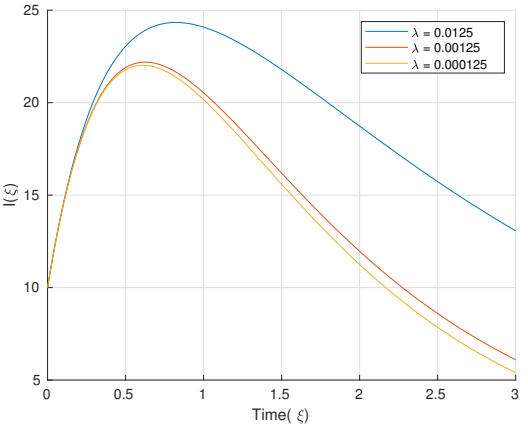

(d) Infected individuals cases rate for different values of λ.

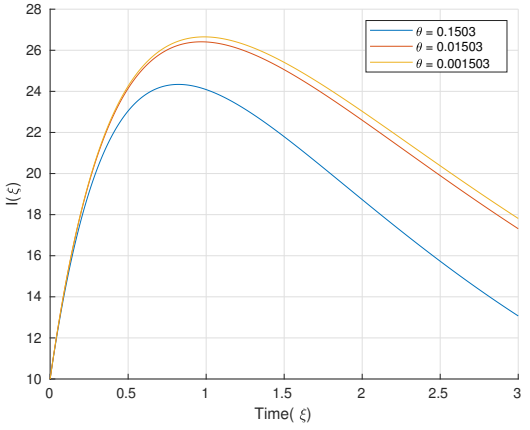

(e) Infected individuals cases rate for different values of θ.

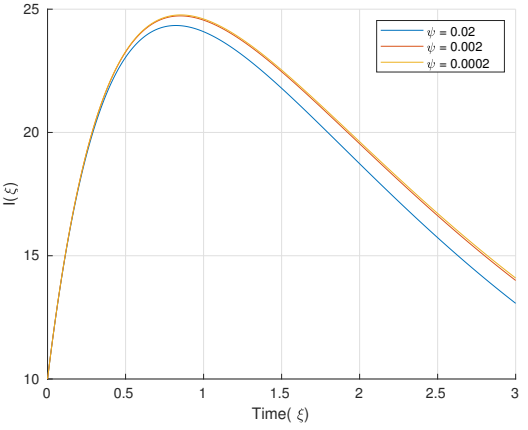

(f) Infected individuals cases rate for different values of ψ.

FIGURE 4. 2-D behviour of infected individuals population for various parameters.

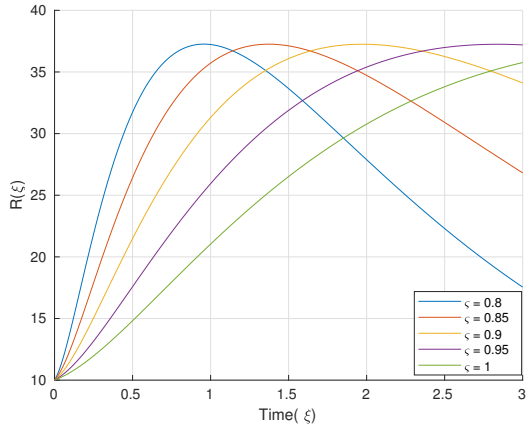

(a) Graphical representation of recovered individuals corresponding to different fractional order of the proposed model.

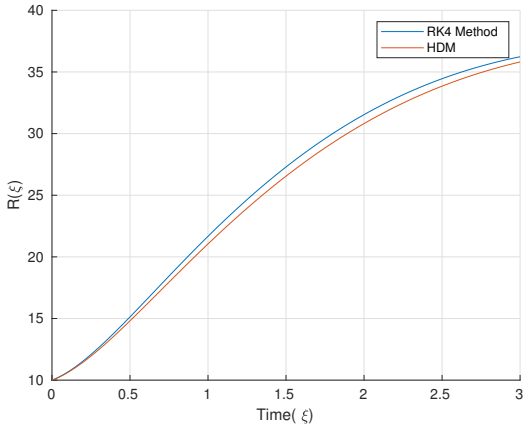

(b) Comparison between our proposed solution up to ten terms with that of RK4 method for recovered individuals of the proposed model.

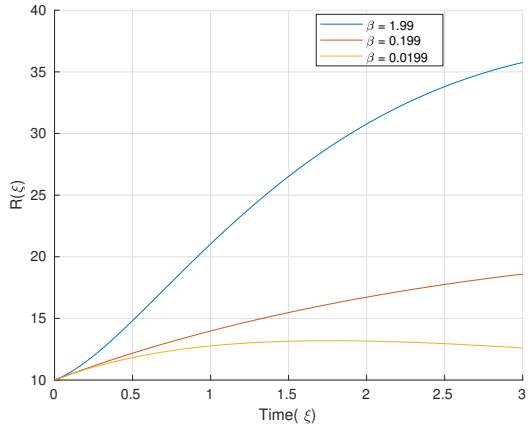

(c) Recovered individuals cases rate for different values of β.

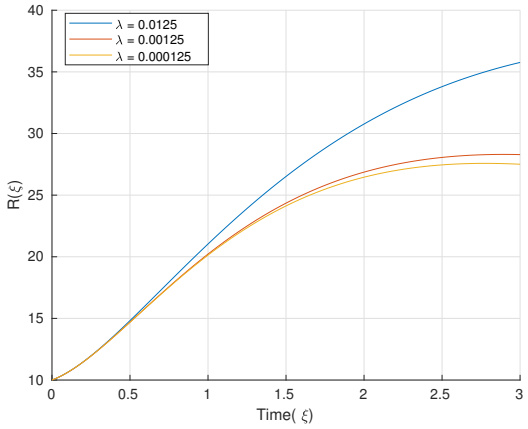

(d) Recovered individuals cases rate for different values of λ.

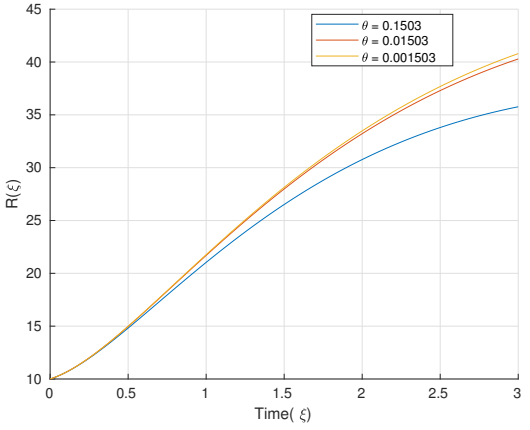

(e) Recovered individuals cases rate for different values of θ.

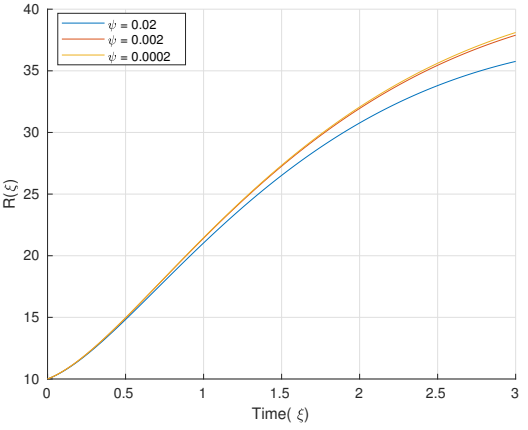

(f) Recovered individuals cases rate for different values of ψ.

FIGURE 5. 2-D behviour of recovered individuals population for various parameters.

8. Conclusions

In this article, we have established criteria to examine typhoid fever models from qualitative and analytical aspects. We have demonstrated the existence and solution of our suggested model by using Banach theorem. To examine the transmission and control dynamics of typhoid fever, we developed an algorithm to obtain semi-analytical solutions for the proposed fractional-order model. The approximate solutions, represented in truncated series form, are illustrated graphically to provide deeper insight into the qualitative behavior of the disease dynamics. Finally, we conclude that the proposed technique is effective in studying biological models in a deeper way. Looking ahead, this research lays a foundation for future investigations into the application of fractional calculus in modeling other infectious diseases characterized by complex dynamics. Further studies may incorporate regional variations, demographic factors, and the impact of emerging interventions such as new vaccines and improved sanitation technologies. Expanding the scope of the current model can deepen the understanding of disease transmission mechanisms and contribute to the development of more effective public health strategies.

Conflict of Interest The authors state that they have no competing interests to declare.

Authors Contribution All the authors made an equal contribution to this paper, and have read and approved the final manuscript.

Funding Information No funds, grants or other support was received.

Ethical Approval No personal or sensitive information is disclosed or compromised.

Data Availability and Access Not applicable.

Acknowledgments The authors express their sincere thanks to the editor and reviewers for their valuable comments and suggestions that improved the quality of the manuscript.

References

[1] P. Aavani and L. J. S. Allen, *The role of CD_4^+ cells in immune system activation and viral reproduction in a simple model for HIV infection*, Appl. Math. Modelling, *75* (2019), 210–222.

[2] F. S. A. Aboubakr, G. M. Ismail, M. M. Khader, M. A. E. Abdelrahman, A. M. T. AbdEl-Bar, and M. Adel, *Derivation of an approximate formula of the Rabotnov fractional-exponential kernel fractional derivative and applied for numerically solving the blood ethanol concentration system*, AIMS Math., *8*(12) (2023), 30704–30716.

[3] H. Abboubakar, A.K. Guidzavai, J. Yangla, I. Damakoa, and R. Mouangue, *Mathematical modeling and projections of a vector-borne disease with optimal control strategies: A case study of the chikungunya in Chad*, Chaos Solitons Fractals, *150* (2021), 111197.

[4] M. Adel, M. M. Khader, and S. Algelany, *High-dimensional chaotic Lorenz system: Numerical treatment using Changhee polynomials of the Appell type*, Fractal Fract., *7*(5) (2023), 398.

[5] M. Adel, M. M. Khader, H. Ahmad, and T. A. Assiri, *Approximate analytical solutions for the blood ethanol concentration system and predator-prey equations by using variational iteration method*, AIMS Math., *8*(8) (2023), 19083–19096.

[6] M. Adel, M. E. Ramadan, H. Ahmad, and T. Botmart, *Sobolev-type nonlinear Hilfer fractional stochastic differential equations with noninstantaneous impulsive*, AIMS Math., *7*(11) (2022), 20105–20125.

[7] Z. J. Ahmed and M. A. Mustafai, *Exploration of vehicle target detection and classification method based on sea lion optimization with deep convolutional neural network*, Journal of Smart Internet of Things, *2022*(1) (2023), 65–80.

[8] M. S. Alam, N. Sharif, and M. H. U. Molla, *Combination of modified Lindstedt-Poincaré and homotopy perturbation methods*, J. Low Freq. Noise Vib. Act. Control, *42*(2) (2022), 642–653.

[9] Z. Alsalami, *Modeling of optimal fully connected deep neural network based sentiment analysis on social networking data*, Journal of Smart Internet of Things, *2022*(1) (2023), 114–132.

[10] S. Alshammari, N. Iqbal, and M. Yar, *Fractional-view analysis of space-time fractional Fokker-Planck equations within Caputo operator*, J. Funct. Spaces, *2022* (2022), Article ID: 4471757.

[11] A. Z. Amin, A. M. Lopes, and I. Hashim, *A space-time spectral collocation method for solving the variable-order fractional Fokker-Planck equation*, J. Appl. Anal. Comput., *13*(2) (2023), 969–985.

[12] R. Agarwal, S. D. Purohit, and Kritika, *A mathematical fractional model with nonsingular kernel for thrombin receptor activation in calcium signalling*, Math. Methods Appl. Sci., *42*(18) (2019), 7160–7171.

[13] K. R. Adeboye and M. Haruna, *A mathematical model for the transmission and control of malaria typhoid co-infection using SIRS approach*, Niger. Res. J. Math., *2*(2) (2015), 1–24.

[14] M. K. Bhan, R. Bahl, and S. Bhatnagar, *Typhoid and paratyphoid fever*, The Lancet, *366*(9487) (2005), 749–762.

[15] E. Bonyah, Z. Hammouch, and M. E. Koksal, *Mathematical modeling of coronavirus dynamics with conformable derivative in Liouville–Caputo sense*, Journal of Mathematics, *2022* (2022), Article ID: 8353343.

[16] T. Butler, *Treatment of typhoid fever in the 21st century: promises and shortcomings*, Clin. Microbiol. Infect., *17*(7) (2011), 959–963.

[17] J. H. Cook, *Are cholera and typhoid vaccines a good investment for a slum in Kolkata, India?*, Ph.D. Dissertation, University of North Carolina at Chapel Hill, (2007).

[18] J. Cook, M. Jeuland, D. Whittington, C. Poulos, J. Clemens, D. Sur, D. D. Anh, M. Agtini, Z. Bhutta, and DOMI, Typhoid Economics Study Group, *The cost-effectiveness of typhoid Vi vaccination programs: calculations for four urban sites in four Asian countries*, Vaccine, *26*(50) (2008), 6305–6316.

[19] J. A. Crump, *Progress in typhoid fever epidemiology*, Clin. Infect. Dis., *68* (2019), 4–9.

[20] E. Demirci, A. Unal, and N. Ozalp, *A fractional order SEIR model with density dependent death rate*, Hacet. J. Math. Stat., *40*(2) (2011), 287–295.

[21] M. Dehghan, J. Manafian, and A. Saadatmandi, *Solving nonlinear fractional partial differential equations using the homotopy analysis method*, Numer. Methods Partial Differential Eq., *26*(4) (2010), 448–479.

[22] M. Dehghan and J. Manafian, *The solution of the variable coefficients fourth-order parabolic partial differential equations by the homotopy perturbation method*, Z. Naturforsch. A, *64*(7–8) (2009), 420–430.

[23] M. Dehghan and J. M. Heris, *Study of the wave-breaking's qualitative behavior of the Fornberg-Whitham equation via quasi-numeric approaches*, Int. J. Numer. Methods Heat Fluid Flow, *22*(5) (2012), 537–553.

[24] R. S. Dubey and P. Goswami, *On the existence and uniqueness analysis of fractional blood glucose-insulin minimal model*, Int. J. Model. Simul. Sci. Comput., *14*(3) (2023), 2350008.

[25] R. S. Dubey, B. S. T. Alkahtani, and A. Atangana, *Analytical solution of space-time fractional Fokker-Plank equation by homotopy perturbation Sumudu transform method*, Math. Probl. Eng., *2015*(1) (2015), 780929.

[26] W. Gao, P. Veeresha, H.M. Baskonus, D. G. Prakasha, and P. Kumar, *A new study of unreported cases of 2019-nCOV epidemic outbreaks*, Chaos Solitons Fractals, *138* (2020), 1–6.

[27] M. M. Gour, L. K. Yadav, S. D. Purohit, and D. L. Suthar, *Homotopy decomposition method to analyze fractional hepatitis B virus infection model*, Appl. Math. Sci. Eng., *31*(1) (2023).

[28] V. Gulkaç, *An extrapolation method for oxygen diffusion problem*, Int. J. Sci. Eng. Res., *6*(4) (2015), 222–226.

[29] V. Gulkaç, *Comparative study between two numerical methods for oxygen diffusion problem*, Commun. Numer. Methods Eng., *25* (2009), 855–863.

[30] J. H. He, *Homotopy perturbation technique*, Comput. Methods Appl. Mech. Eng., *178* (1999), 257–262.

[31] B. K. Hussan, Z. N. Rashid, S. R. Zeebaree, and R. R. Zebari, *Optimal deep belief network enabled vulnerability detection on smart environment*, Journal of Smart Internet of Things, *2023* (2023), 146–162.

[32] Y. F. Ibrahim, S. E. Abd El-Bar, M. M. Khader, and M. Adel, *Studying and simulating the fractional COVID-19 model using an efficient spectral collocation approach*, Fractal Fract., *7*(4) (2023), 307.

[33] B. Ivanoff, M. M. Levine, and P. Lambert, *Vaccination against typhoid fever: Present status*, Bull. World Health Organ., *72*(6) (1994), 957.

[34] I. E. Khan, S. Mustafa, A. Shokri, S. Li, A. Akgul, and A. Bariq, *The stability analysis of a nonlinear mathematical model for typhoid fever disease*, Sci. Rep., *13*(1) (2023), 15284.

[35] M. A. Khan, M. Alhaisoni, M. Nazir, A. Alqahtani, A. Binbusayyis, S. Alsubai, Y. Nam, and B. G. Kang, *A healthcare system for COVID-19 classification using multi-type classical features selection*, CMC, Comput. Mater. Continua, *74*(1) (2023), 1393–1412.
[36] M. L. G. Kuniyoshi and F. L. Pio dos Santos, *Mathematical modelling of vector-borne diseases and insecticide resistance evolution*, J. Venom. Anim. Toxins Trop. Dis., *23* (2017), 34.
[37] J. Manafian and M. Lakestani, *Exact solutions for the integrable sixth-order Drinfeld–Sokolov–Satsuma–Hirota system by analytical methods*, Int. Sch. Res. Notices, *2014* (2014), Article ID 840689, 1–8.
[38] J. Manafian, M. Lakestani, and A. Bekir, *Comparison between the generalized tanh–coth method and the* (G'/G)*-expansion method for solving NPDEs and NODEs*, Pramana – J. Phys., *87*(6) (2016), 1–14.
[39] J. Mann and M. Roberts, *Modelling the epidemiology of hepatitis B in New Zealand*, J. Theor. Biol., *269*(1) (2011), 266–272.
[40] J. E. Meiring, F. Khanam, B. Basnyat, et al., *Typhoid fever*, Nat. Rev. Dis. Primers, *9*(71) (2023).
[41] G. G. Mohammed and Z. Zaheer, *NeuroCyberGuard: Developing a robust cybersecurity defense system through deep neural learning-based mathematical modeling*, Journal of Smart Internet of Things, *2023*(2) (2023), 133–145.
[42] S. S. Musa, S. Zhao, N. Hussaini, S. Usaini, and D. He, *Dynamics analysis of typhoid fever with public health education programs and final epidemic size relation*, Results Appl. Math., *10* (2021), 100153.
[43] A. Naghipour and J. Manafian, *Application of the Laplace Adomian decomposition and implicit methods for solving Burgers' equation*, TWMS J. Pure Appl. Math., *6*(1) (2015), 68–77.
[44] E. F. Nsutebu, P. Martins, and D. Adiogo, *Prevalence of typhoid fever in febrile patients with symptoms clinically compatible with typhoid fever in Cameroon*, Trop. Med. Int. Health, *8*(6) (2003), 575–578.
[45] J. K. Nthiiri, *Mathematical modelling of typhoid fever disease incorporating protection against infection*, Br. J. Math. Comput. Sci., *14*(1) (2016), 1–10.
[46] V. E. Pitzer, C. C. Bowles, S. Baker, G. Kang, V. Balaji, J. J. Farrar, and B. T. Grenfell, *Predicting the impact of vaccination on the transmission dynamics of typhoid in South Asia: a mathematical modeling study*, PLoS Negl. Trop. Dis., *8*(1) (2014), e2642.
[47] I. Podlubny, *Fractional differential equations*, Math. Sci. Eng., *198*, Academic Press, San Diego, (1999).
[48] S. Pourghanbar, J. Manafian, M. Ranjbar, A. Aliyeva, and Y. S. Gasimov, *An efficient alternating direction explicit method for solving a nonlinear partial differential equation*, Math. Probl. Eng., (2020), Article ID: 9647416, 12 pages.
[49] A. K. Schemmer, *Heterogeneity of inflammation and host metabolism in a typhoid fever model*, Doctoral dissertation, University of Basel, (2012).
[50] A. K. Shakir, *Optimal deep learning driven smart sugarcane crop monitoring on remote sensing images*, Journal of Smart Internet of Things, *2022*(1) (2023), 163–177.
[51] N. Sharif, M. S. Alam, and H. U. Molla, *Dynamics of nonlinear pendulum equations: Modified homotopy perturbation method*, J. Low Freq. Noise Vib. Act. Control, (2025).
[52] M. Shrahili, R. S. Dubey, and A. Shafay, *Inclusion of fading memory to Banister model of changes in physical condition*, Discrete Contin. Dyn. Syst., *13*(3) (2018), 881–888.
[53] S. Thornley, C. Bullen, and M. Roberts, *Hepatitis B in a high prevalence New Zealand population: a mathematical model applied to infection control policy*, J. Theor. Biol., *254*(3) (2008), 599–603.
[54] World Health Organization, *Typhoid vaccines: WHO position paper*, Wkly Epidemiol. Rec., *83* (2008), 49–59.
[55] H. Ye and Y. Ding, *Nonlinear dynamics and chaos in a fractional-order HIV model*, Math. Probl. Eng., *2009* (2009), Article ID: 78614.